Journal of Electrical and Computer Engineering Innovations
(JECEI)
Journal homepage: http://www.jecei.sru.ac.ir

Research paper

A Differential Microstrip Resonator-ased Sensor for High-Sensitivity Moisture Detection in Wheat Grains

Abolfazl Bijari [*], ***Sara Nooki***

Faculty of Electrical and Computer Engineering, University of Birjand, Birjand, Iran.

Article Info

Article History:
Received 03 July 2025
Reviewed 17 August 2025
Revised 04 September 2025
Accepted 11 October 2025

Keywords:
Differential measurement,
Moisture content (MC)
Sensor
Microstrip
Transmission zero (TZ)

[*]Corresponding Author's Email Address: *a.bijari@birjand.ac.ir*

Abstract

Background and Objectives: Accurate measurement of moisture content (MC) in wheat grains is vital for quality control and storage management. This study presents the development of a differential microwave sensor with enhanced sensitivity for detecting MC in wheat grains, leveraging resonant techniques to improve detection precision.

Methods: The proposed sensor utilizes two identical half-wavelength ($\lambda/2$) microstrip resonators symmetrically coupled to a standard 50Ω transmission line. One resonator serves as a reference with a relative permittivity ($\acute{\epsilon}_r$) of 1, while the second is exposed to the sample under test (SUT), where $\acute{\epsilon}_r > 1$. This differential structure enables the identification of dielectric property changes due to moisture variation. The operating principles are theoretically analyzed using even- and odd-mode techniques.

Results: The proposed sensor exhibits three distinct transmission zeros (TZs) within the 0.1–2 GHz frequency range, which arise from the harmonic behavior of the resonators. A prototype was fabricated on a low-cost, compact substrate with dimensions of 6 × 4.5 × 0.16 cm³ and was experimentally tested, confirming the simulation results. The sensor demonstrates a high normalized sensitivity of 7.63%.

Conclusion: The developed differential microwave sensor demonstrates strong potential for precise and reliable MC detection in wheat grains. Its compact design, cost-effectiveness, and high sensitivity make it a suitable candidate for practical agricultural and food monitoring applications.

How to cite this paper:
A. Bijari, S. Nooki, "A differential microstrip resonator-ased sensor for high-sensitivity moisture detection in wheat grains," J. Electr. Comput. Eng. Innovations, 14(1): 231-240, 2026.

DOI: 10.22061/jecei.2025.12218.861

URL: https://jecei.sru.ac.ir/article_2429.html

Introduction

Real-time monitoring of moisture content (MC) plays a vital role across a wide spectrum of industries, including agriculture [1], food processing [2], construction [3], biomedical engineering [4], and logistics [5]. In agricultural applications, particularly in cereal grain production, accurate and timely MC measurements are essential for optimizing harvesting schedules, controlling drying processes, and ensuring safe long-term storage. Improper moisture levels can lead to microbial spoilage, quality degradation, and substantial economic loss [2]. Conventional methods such as oven-drying remain the standard reference technique due to their accuracy; however, these methods are inherently destructive, labor-intensive, and time-consuming, making them unsuitable for high-throughput or in-situ applications. To address these limitations, researchers have increasingly turned to electromagnetic (EM) sensing, particularly microwave-based techniques, which offer non-destructive, real-time monitoring capabilities. These methods exploit the sensitivity of dielectric properties to moisture variation, as water exhibits a significantly higher relative permittivity than dry organic matter.

Various microwave sensing techniques have been employed, including planar microstrip transmission lines [1], [3], [6], [7], cavity resonators and waveguides [5], [8], [9], and free-space antenna-based systems [10], [11]. Among these, planar microstrip resonator-based sensors are especially attractive due to their compact size, ease of fabrication using printed circuit board (PCB) technology, strong EM field confinement, and potential for integration into low-cost, portable measurement systems.

The core sensing mechanism in microwave resonators relies on detecting shifts in resonance frequency resulting from changes in the effective dielectric constant of the material under test. As moisture increases in a dielectric medium such as grain, the overall permittivity rises, causing a downward shift in the resonator's frequency response. Several notable studies have demonstrated the viability of this principle. For example, Jain et al. [12] developed a U-shaped microstrip patch antenna operating at 5.2 and 6.8 GHz for MC measurement in basmati rice, achieving a mean relative error of 0.55% within a moisture range of 10.7–21.9%. Similarly, Javanbakht et al. [13] implemented a flexible frequency-selective surface incorporating square complementary split-ring resonators, observing a 160 MHz frequency shift as barley MC increased from 10% to 25%. Mun et al. [14] designed wide-ring and coupled-line resonators for rice grain analysis, reporting frequency shifts of 4.36 and 10.69 MHz per 1% MC change with a prediction error between 0.85% and 1.30%. In another approach, Kapoor et al. [15] utilized an interdigital capacitor integrated with a planar electric–LC (ELC) resonator, achieving a normalized sensitivity of 5.1% through electric field concentration within the sensing region. Despite these advancements, many existing designs employ single-ended configurations, which are inherently susceptible to common-mode disturbances such as temperature variations, mechanical deformation, or environmental noise. For enhanced robustness and accuracy, differential sensor architectures are increasingly gaining attention. These configurations compare responses from a sensing element and a reference structure, effectively suppressing common-mode effects and improving measurement reliability. In this paper, a highly sensitive differential microwave sensor is proposed based on planar microstrip resonators for precise MC detection in wheat grains, which is recognized as the world's second-most cultivated cereal crop [16]. The proposed sensor employs a pair of $\lambda/2$ resonators, one operating as a reference and the other exposed to the sample under test (SUT), enabling differential measurement with improved immunity to external disturbances.

The remainder of this paper is organized as follows: the sensor design methodology, including theoretical modeling using even- and odd-mode analysis, is described. Experimental results and validation are then presented, highlighting the sensor's performance metrics. The paper concludes with a summary of findings and outlines potential applications in agricultural sensing and quality monitoring.

Proposed Sensor Theory

Fig. 1 depicts the schematic of the proposed microwave sensor, which employs a differential sensing scheme based on two identically designed half-wavelength ($\lambda/2$) microstrip resonators. These resonators are symmetrically positioned on either side of a central 50 Ω microstrip transmission line and are excited through gap coupling. One resonator operates as the sensing element exposed to the SUT, while the other serves as a reference element, shielded from the sample. This configuration enhances measurement reliability by suppressing the influence of environmental perturbations such as temperature fluctuations, moisture changes, and mechanical instabilities.

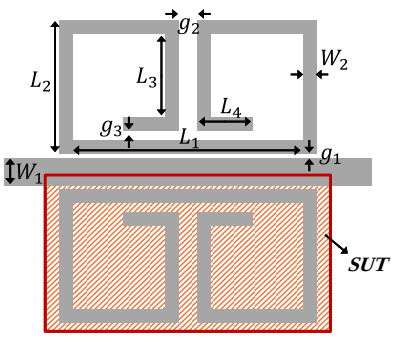

Fig. 1: Proposed microwave moisture sensor.

A. Sensor Design

In the absence of a sample (unloaded condition), both resonators exhibit identical EM behavior, producing coincident resonance frequencies and overlapping transmission zeros (TZs). When a dielectric sample is introduced above the sensing resonator, its effective permittivity increases, resulting in a shift of the corresponding TZ. In contrast, the reference resonator maintains a stable frequency response, allowing differential detection of changes solely attributable to the sample's MC.

The proposed sensor is fabricated on a low-cost FR-4 substrate, selected for its widespread availability, ease of PCB processing, and suitable dielectric properties (thickness = 1.6 mm, ε_r = 4.3, and tanδ = 0.02). This substrate provides a favorable balance between performance and manufacturing cost, making the sensor practical for scalable deployment in agricultural moisture sensing applications. The sensor's structural symmetry enables the transmission coefficient (S_{21}) to be expressed in terms of odd- and even-mode input impedances as follows [17]:

$$S_{21} = \frac{Z_1(Z_{in,e} - Z_{in,o})}{(Z_{in,e} + Z_1)(Z_{in,o} + Z_1)} \quad (1)$$

where $Z_{in,o}$ and $Z_{in,e}$ are the odd- and even-mode input impedances of the sensor structure and Z_1 = 50 Ω represents the characteristic impedance of the feed line. The TZ condition, characterized by a complete suppression of signal transmission (S_{21} = 0), occurs when the input impedances under odd- and even-mode excitations become identical, that is, when $Z_{in,o}$ = $Z_{in,e}$. This condition signifies destructive interference between the modes, leading to the formation of a notch or zero in the transmission spectrum. As illustrated in Fig. 2(a), the odd- and even-mode impedances are obtained by applying appropriate boundary conditions along the plane of symmetry of the sensor structure.

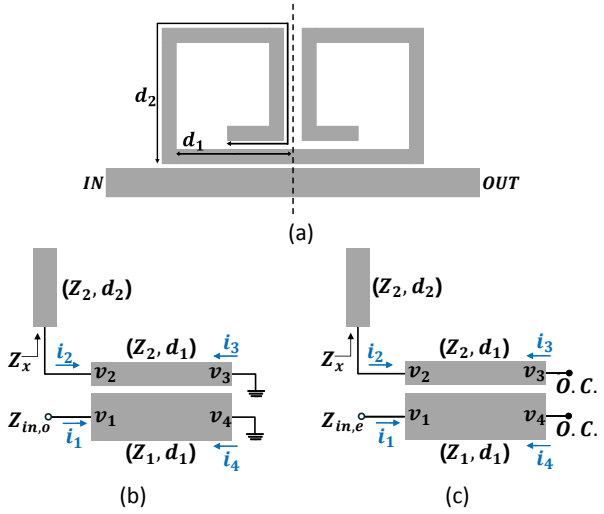

Fig. 2: (a) EW and MW boundaries of the sensor with equivalent model for (b) Odd-mode and (c) Even-mode.

Specifically, an electric wall (EW) is imposed for the odd-mode excitation, enforcing a virtual open circuit along the symmetry axis. Conversely, a magnetic wall (MW) is applied for the even-mode excitation, corresponding to a virtual short circuit along the same axis. For both odd- and even-mode excitations, the input impedance $Z_{in,o,e} = v_1/i_1$ can be obtained using the equivalent circuit models shown in Figs. 2(b) and 2(c), respectively, as follows:

$$[v]_{4\times1} = [Z]_{4\times4} \cdot [i]_{4\times1} \quad (2)$$

here, [Z] denotes the impedance matrix of the asymmetrically coupled transmission line, with its elements defined as [18], [19]:

$$Z_{11} = Z_{44} = -j\left(\frac{Z_{c1}R_\pi - Z_{\pi1}R_c}{R_\pi - R_c}\right)\cot\beta d_1 \quad (3)$$

$$Z_{12} = Z_{21} = Z_{34} = Z_{43} = j\left(\frac{Z_{c2} - Z_{\pi2}}{R_\pi - R_c}\right)\cot\beta d_1 \quad (4)$$

$$Z_{13} = Z_{31} = Z_{24} = Z_{42} = -j\left(\frac{Z_{c1} - Z_{\pi1}}{R_\pi - R_c}\right)R_\pi R_c \csc\beta d_1 \quad (5)$$

$$Z_{14} = Z_{41} = -j\left(\frac{Z_{c1}R_\pi - Z_{\pi1}R_c}{R_\pi - R_c}\right)\csc\beta d_1 \quad (6)$$

$$Z_{22} = Z_{33} = j\left(\frac{Z_{c2}R_c - Z_{\pi2}R_\pi}{R_\pi - R_c}\right)R_\pi R_c\cot\beta d_1 \quad (7)$$

$$Z_{23} = Z_{32} = -j\left(\frac{Z_{c1}R_c - Z_{01\pi}R_\pi}{R_\pi - R_c}\right)R_\pi R_c \csc\beta d_1 \quad (8)$$

where Z_c and Z_π represent the characteristic impedances of the common-mode (c-mode) and differential-mode (π-mode) in the asymmetric coupled-line structure, respectively. R_c and R_π denote the corresponding mode-voltage ratios, and β is the phase constant. Using (2) and applying the relation $v_2 = -Z_X i_2$, the odd- and even-mode input impedances can be derived, where Z_X the stub impedance seen at the node of v_2, and is expressed as:

$$Z_x = -jZ_2 cot(\beta_2 d_2) \quad (9)$$

where Z_2 is the characteristic impedance and the phase constants of the $\lambda/2$ resonator. Based on theoretical analysis with Z_2 = 70 Ω, g_1 = 0.2 mm, and d_1 = 20 mm, Fig. 3(a) illustrates the sensor's frequency response.

Three TZs are seen within the 0.1–2 GHz frequency range. When d_2 is set to 60 mm, the first TZ appears at 0.55 GHz, corresponding to the fundamental mode of the half-wavelength ($\lambda/2$) resonator. The second and third TZs are located at 1.1 GHz and 1.65 GHz, respectively, representing higher-order resonant modes. As shown in Fig. 3(b), all TZs exhibit a downward frequency shift with increasing dielectric constant of the

SUT, due to the enhanced effective permittivity experienced by the sensing resonator. Based on the dimensional configuration illustrated in Fig. 1 and Fig. 2(a), and taking into account the characteristic impedances of the transmission lines as well as the requirement for maximum coupling efficiency, the sensor prototype was carefully designed and optimized. The finalized geometric parameters (all units in mm) are as follows: L_1 = 36.8, L_2 = 20.5, L_3 = 14.7, L_4 = 8, W_1 = 3.2, W_2 = 1.6, g_1 = 0.2, g_2 = 3, and g_3 = 1.

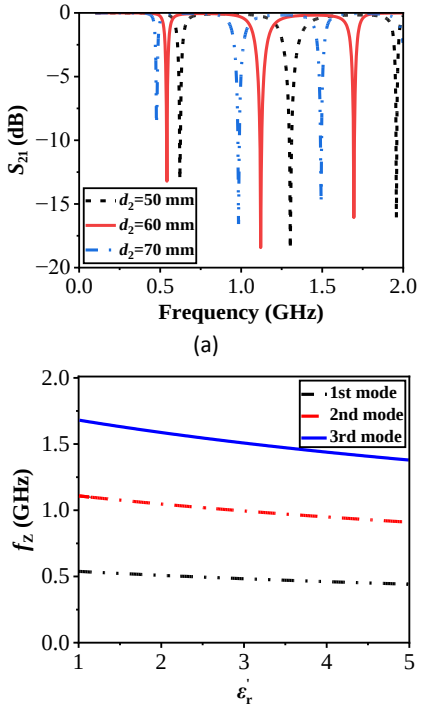

Fig. 3: (a) Simulated frequency response of the proposed sensor. (b) TZ shift versus dielectric constant of the SUT ($\acute{\varepsilon}_r$).

B. Sensitivity Analysis

Sensitivity is a critical performance metric for evaluating the effectiveness of microwave sensors in detecting dielectric changes. Since the positions of the TZs are directly influenced by the dielectric constant of the SUT ($\acute{\varepsilon}_r$), the absolute sensitivity (S) and normalized sensitivity (S_n) of the sensor can be defined as follows:

$$S = \left|\frac{df_z}{d\varepsilon_r'}\right| = \left|\frac{df_z}{d\varepsilon_{eff}} \times \frac{d\varepsilon_{eff}}{d\varepsilon_r'}\right| \tag{10}$$

$$S_n = \frac{1}{f_z}\left|\frac{df_z}{d\varepsilon_r'}\right| \tag{11}$$

where f_z is the TZ frequency, and the effective dielectric constant (ε_{eff}) of the sensing region is given by [20]:

$$\varepsilon_{\text{eff}} = q_1\varepsilon_{\text{r}} + q_2\varepsilon_r' \tag{12}$$

where q_1 and q_2 are the dielectric filling fractions that represent the proportional contributions of the substrate and the SUT, respectively, and ε_{r} denotes the relative permittivity of the substrate. By substituting (12) into (10) and (11), and assuming that the TZ frequencies correspond to the resonant frequencies of a half-wavelength ($\lambda/2$) resonator, the absolute sensitivity and normalized sensitivity of the proposed sensor can be expressed as:

$$S = \frac{ncq_2}{4d_T\varepsilon_{eff}^{3/2}} = \frac{ncq_2}{4d_T(q_1\varepsilon_{\text{r}} + q_2\varepsilon_r')^{\frac{3}{2}}} \tag{13}$$

$$S_n = \frac{q_2}{2\varepsilon_{eff}} = \frac{q_2}{2(q_1\varepsilon_{\text{r}} + q_2\varepsilon_r')} \tag{14}$$

where n denotes the harmonic order, c is the speed of light in vacuum, and $d_T = 2(d_1 + d_2)$ represents the total length of the resonant path. Fig. 3(b) validates the analytical expression in (13), confirming that higher-order harmonic modes exhibit increased absolute sensitivity due to their stronger frequency dependence on the dielectric properties of the SUT. Furthermore, as indicated by (14), the normalized sensitivity remains independent of the harmonic order, making it a more consistent metric for performance comparison across different frequency bands.

To quantitatively evaluate the sensitivity of the proposed sensor, a series of full-wave EM simulations was carried out using CST Studio Suite. These simulations were performed over a range of hypothetical relative permittivity values assigned to the SUT. The resulting transmission spectra clearly show the shifts in the positions of the TZs in response to changes in the SUT's dielectric constant. The frequency responses corresponding to different permittivity levels are presented in Fig. 4, demonstrating the sensor's capability to detect subtle dielectric variations through distinct TZ displacements.

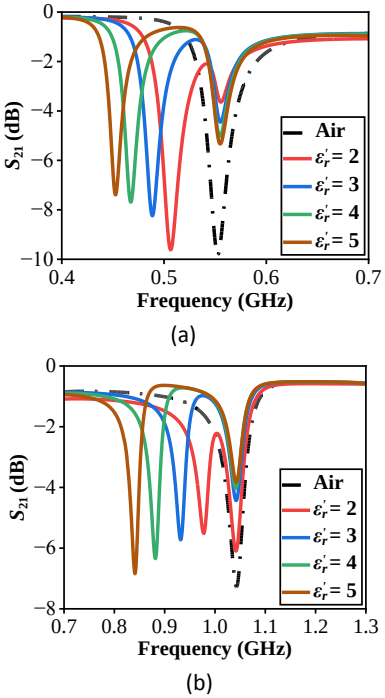

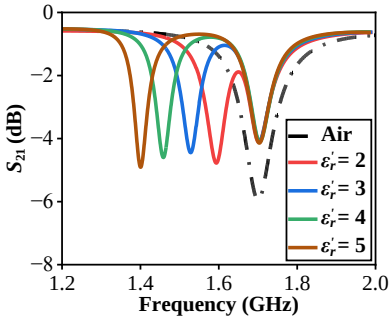

(c)

Fig. 4: EM Simulated response of the first three modes with/without SUT on one resonator (dashed: no SUT).

Since sensors designed for MC measurement may operate at different frequency bands, a fair performance comparison requires the use of an averaged normalized sensitivity metric. The average normalized sensitivity ($S_{n,ave}$) is defined as:

$$S_{n,ave}(\%) = Average\left\{\frac{1}{f_{ref}}\frac{(f_{ref} - f_{SUT})}{(\varepsilon'_{r_{SUT}} - 1)}\right\} \times 100 \quad (15)$$

According to Fig. 4, although the third mode demonstrates the highest absolute sensitivity due to its higher frequency, the average normalized sensitivities for the first, second, and third modes of the proposed sensor are calculated to be 5.98%, 5.35%, and 5.21%, respectively.

Experimental Results and Discussion

A prototype of the proposed sensor, with dimensions specified in the previous section, was fabricated and is shown in Fig. 5(a). The overall sensor size is $6 \times 4.5 \times 0.16$ cm³, implemented on an FR-4 substrate. To facilitate practical handling and consistent placement of the SUT, a custom plexiglass frame was designed, as illustrated in Fig. 5(b). The frame securely encloses all four edges of the sensor and features a movable wall mechanism, enabling precise and repeatable positioning of the SUT over the sensing resonator. Experimental validation confirmed that the presence of the plexiglass fixture introduces negligible influence on the sensor's EM performance.

Fig. 6 illustrates the experimental measurement setup, which employed an Agilent 8720C vector network analyzer (VNA) to characterize the proposed sensor under both unloaded conditions and with wheat grain samples at MC levels of 10%, 20%, and 30%.

It should be noted that variations in kernel size influence the packing density and, consequently, the effective dielectric path length within the SUT. Larger kernels can create interstitial air gaps between grains, leading to a reduction in the measured dielectric constant, whereas smaller kernels tend to pack more densely, increasing the apparent dielectric constant.

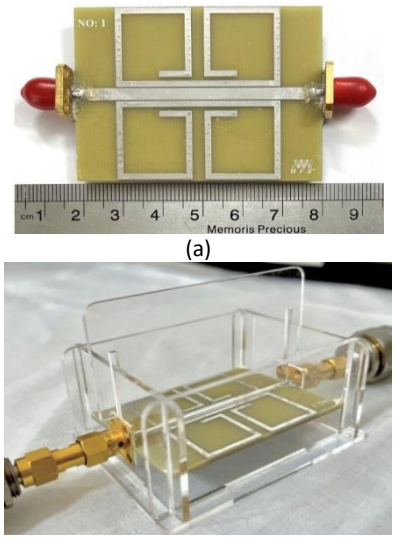

(a)

(b)

Fig. 5: (a) Fabricated sensor prototype. (b) Plexiglass frame for accurate positioning of the SUT.

Moreover, wheat husks generally contain less water and exhibit dielectric properties distinct from the kernels. The presence of husks can therefore lower the effective dielectric constant, potentially causing an underestimation of the true MC. To ensure accurate measurements, microwave moisture sensors must be calibrated using samples that reflect the anticipated grain population, including inherent heterogeneities. Accordingly, all wheat samples used in this study were collected from a specific region in Iran, carefully dehusked, and selected to achieve near-uniform kernel size.

To achieve specific MC levels, bulk wheat samples were conditioned by soaking in water for different durations, followed by controlled drying. The actual MC of each batch was then precisely determined using the ASAE S352 standard method [21], which is an internationally recognized reference technique for grain moisture measurement.

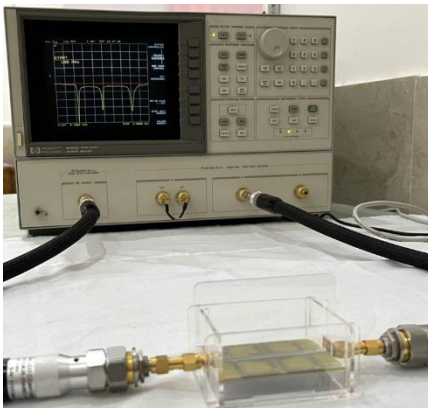

(a)

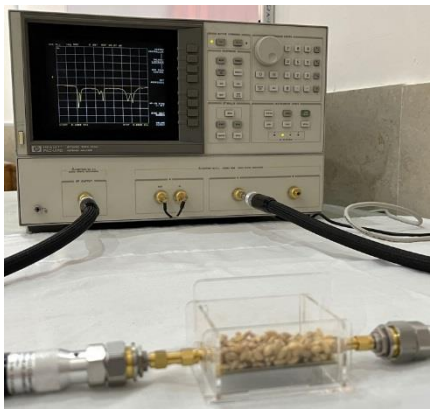

(b)

Fig. 6: (a) Measurement setup using VNA: (a) Sensor in the unloaded condition, (b) Sensor loaded with the wheat sample.

This procedure was repeated several times to ensure accuracy and repeatability, and ultimately, samples with stable MC levels of approximately 10%, 20%, and 30% were prepared. As an illustration, Fig. 7 illustrates one of the conditioning steps where multiple wheat samples were placed in a laboratory oven to regulate their MC. During measurements, a fixed volume of 8 g of wheat was consistently used as the SUT, selected to completely cover the sensing resonator and to minimize air gaps between grains due to their granular structure. Although higher-MC samples exhibited slightly greater thickness when placed on the sensor, its influence on the sensor response was negligible. To further ensure uniform contact between the grains and the sensor surface, a sterilized clamp was employed to evenly distribute the samples.

Fig. 7: Experimental setup for MC determination according to the ASAE S352 standard.

The measured and simulated transmission responses corresponding to each TZ are presented individually in Fig. 8. Moreover, multiple full-wave EM simulations were performed to estimate the effective relative permittivity of the wheat grain samples. The simulated responses were compared with the measured data, as shown in Fig. 9. Based on this comparison, the extracted relative permittivity values were approximately 1.8 for 10% MC, 2.1 for 20% MC, and 2.7 for 30% MC.

Accordingly, the relationship between frequency and MC for each mode can be described in the general form as follows:

$$f_{zn} = f_{zn0} - \alpha_n MC \tag{16}$$

where f_{zn} is the n-th mode frequency at a given MC, f_{zn0} is the resonance frequency in the dry condition, and α_n is the experimentally extracted sensitivity coefficient. These calibration equations confirm that the three resonant modes can be mathematically and experimentally mapped to the MC.

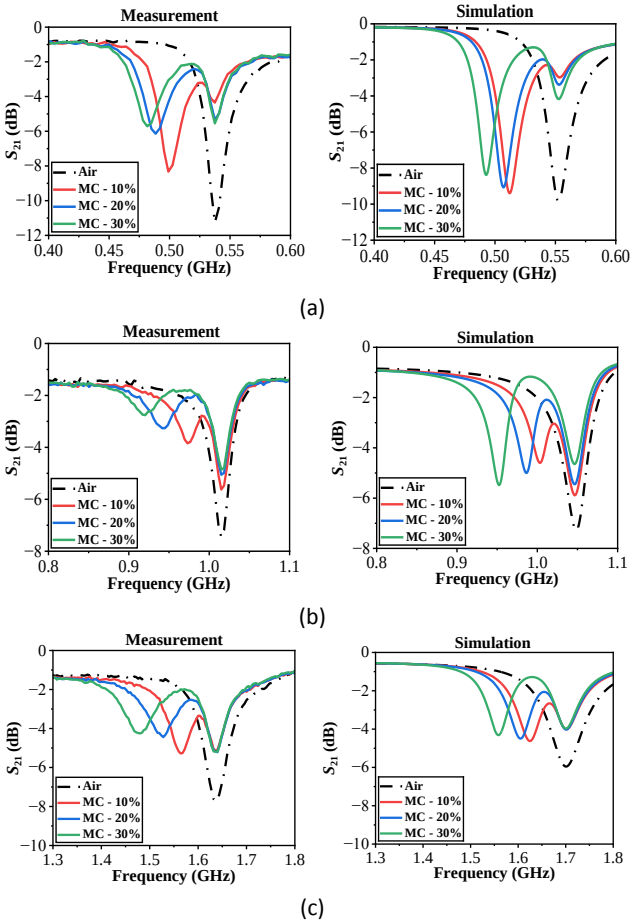

Fig. 8: Measurement and simulation results for the frequency response of the sensor's first three modes.

Based on the measurement results presented in Fig. 8 and Fig. 9, the average normalized sensitivities of the proposed sensor are calculated to be 7.63%, 5.78%, and 5.69% for the first, second, and third modes, respectively. Like most dielectric-based microwave sensors, the proposed design requires calibration for different grain types because the dielectric properties of agricultural products depend not only on MC but also on intrinsic factors such as density, composition, and porosity.

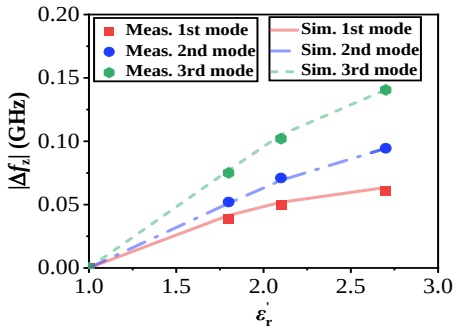

Fig. 9: Comparison of sensing curves from EM simulations and measured TZ shifts versus the SUT's dielectric constant.

In this study, calibration was performed for wheat following the ASAE S352 standard method [21]; therefore, the extracted permittivity values shown in Fig. 9 correspond to wheat samples at known MC levels. For other cereals (e.g., rice, barley, corn), the same calibration procedure must be repeated to establish the empirical mapping between MC and effective permittivity ($\acute{\epsilon}_r$). The underlying principle remains unchanged: Equations (13) and (14) provide the general theoretical relation between the sensitivity and the dielectric constant of the SUT. Thus, although the sensor structure is universal, reliable use with other grain types requires a one-time calibration curve to account for material-specific dielectric characteristics.

To emphasize the sensitivity performance of the proposed design, the average normalized sensitivity ($S_{n,ave}$) is benchmarked against previously reported sensors. A summary of the comparative results is provided in Table 1.

Table 1: Comparison of the proposed sensor with other works

Ref.	f_{ref} (GHz)	$S_{n,ave}$ (%)	Substrate	SUT	Diff.
[1]	4.5	2.5	FR-4	Soil	Yes
[14]	2.44	5.5	RT/Duroid 5880	Rice	No
[22]	2.1	3.4	RO4350	Dielectric slabs	Yes
[23]	2.41	3.73	RO4350	Dielectric slabs	Yes
[24]	2.18	4.03	RT6002	Dielectric slabs	Yes
[12]	5.2	2.249	FR-4	Rice	No
[25]	3.364	4.915	Taconic TLY-5	Wood	Yes
[26]	2.5875	2.21	RO4350B	Dielectric slabs	Yes
[27]	2.56	1.23	RO4350B	Ethanol	No
[28]	1.811	0.76	RO4003C	Ethanol	Yes
[29]	2.4	2	F4B	Leaf	No
[30]	5.318	4.98	RF-35	Dielectric slabs	No
This work	0.54 1.01 1.63	7.63 5.78 5.69	FR-4	Wheat grains	Yes

Diff: Differential structure

The results indicate that the proposed sensor demonstrates superior normalized sensitivity compared to previously reported designs. In addition, the use of a low-cost FR-4 substrate enhances the sensor's practicality and cost-effectiveness, making it a promising candidate for quality control applications in the food industry, particularly for real-time MC monitoring in grain storage and processing environments.

Effects of Non-Ideal Factors

The differential architecture of the proposed sensor was selected to suppress common-mode effects such as ambient temperature and humidity. However, both air and SUT show temperature-dependent permittivity, with lower temperatures slightly increasing wheat MC and its relative permittivity ($\acute{\epsilon}_r$), and higher temperatures decreasing them [31]. Due to limited laboratory facilities, these effects were simulated in the EM analysis by varying dielectric properties for ±5 °C in ambient temperature and ±10% changes in ambient humidity. Fig. 10 shows the results at different MC levels.

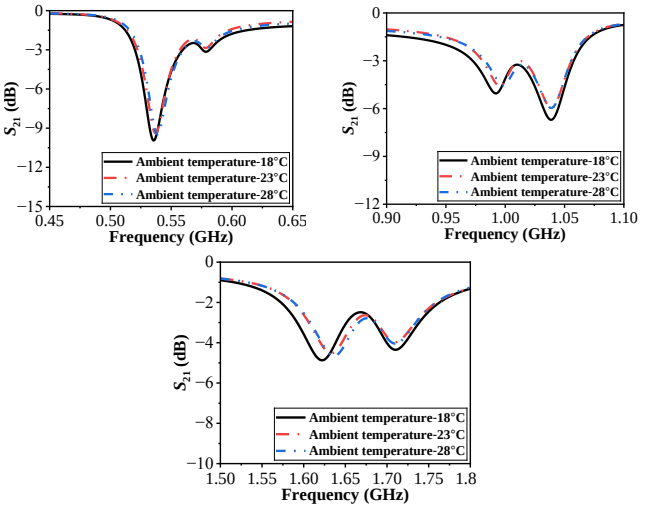

(a)

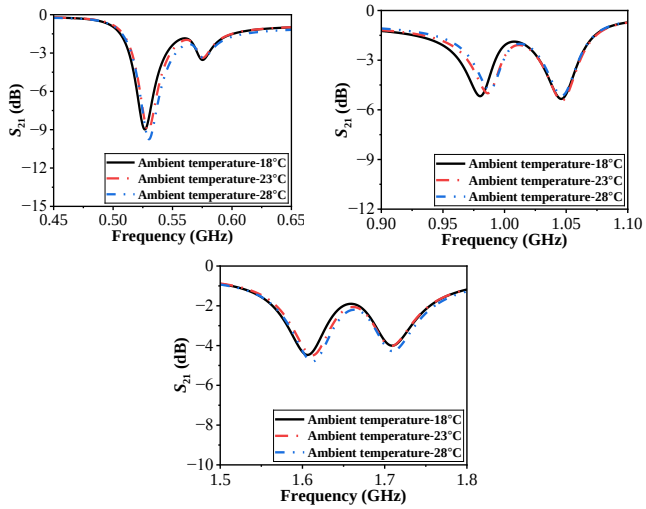

(b)

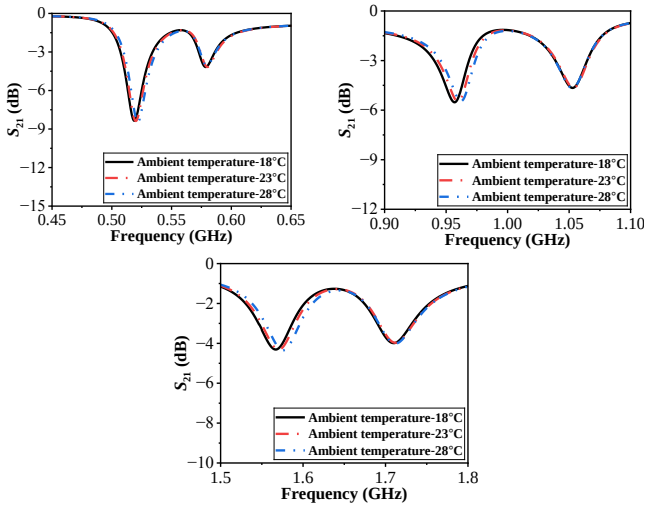

(c)

Fig. 10: Simulation results of ambient temperature variation for wheat grains at different MCs: (a) 10%, (b) 20%, (c) 30%.

As can be seen in Fig. 10, relative to room temperature (23 °C), the dielectric constant showed a nearly symmetric variation: increasing by about +1.5% at 18 °C and decreasing by approximately –1.5% at 28 °C. This corresponds to a temperature sensitivity of ~0.003 units/°C, indicating that the dielectric response remains moderately stable around room temperature, with less than 2% relative error across the tested range of thermal fluctuations. The corresponding relative permittivity from the simulation is obtained and summarized in Table 2.

Table 2: Relative permittivity ($\acute{\epsilon}_r$) of wheat at various MCs and ambient temperatures

MC%	$\acute{\epsilon}_r$ @ 18∘C	$\acute{\epsilon}_r$ @ 23∘C	$\acute{\epsilon}_r$ @ 28∘C
10%	1.827	1.8	1.773
20%	2.132	2.1	2.069
30%	2.741	2.7	2.660

Moreover, to evaluate the effect of ambient humidity, an average environmental humidity of approximately 35% at a temperature of 23 °C was considered. Since variations in ambient humidity can influence the MC of the SUTs, a ±10% change in relative ambient humidity was simulated as illustrated in Fig. 11. The corresponding variations in the dielectric constant of wheat samples are summarized in Table 3.

It should be noted that the relationship between ambient humidity and grain MC is nonlinear. As shown in Table 3, the relative permittivity ($\acute{\epsilon}_r$) of wheat increases with both MC and ambient humidity, but the rate of change is not uniform across conditions. At lower initial MC levels, grains absorb moisture more readily with increases in relative ambient humidity.

Table 3: Relative permittivity ($\acute{\epsilon}_r$) of wheat at various MCs and ambient humidity levels

MC%	Ambient humidity @ 25%	Ambient humidity @ 35%	Ambient humidity @ 45%
10%	1.64	1.8	1.95
20%	1.92	2.1	2.28
30%	2.22	2.7	2.88

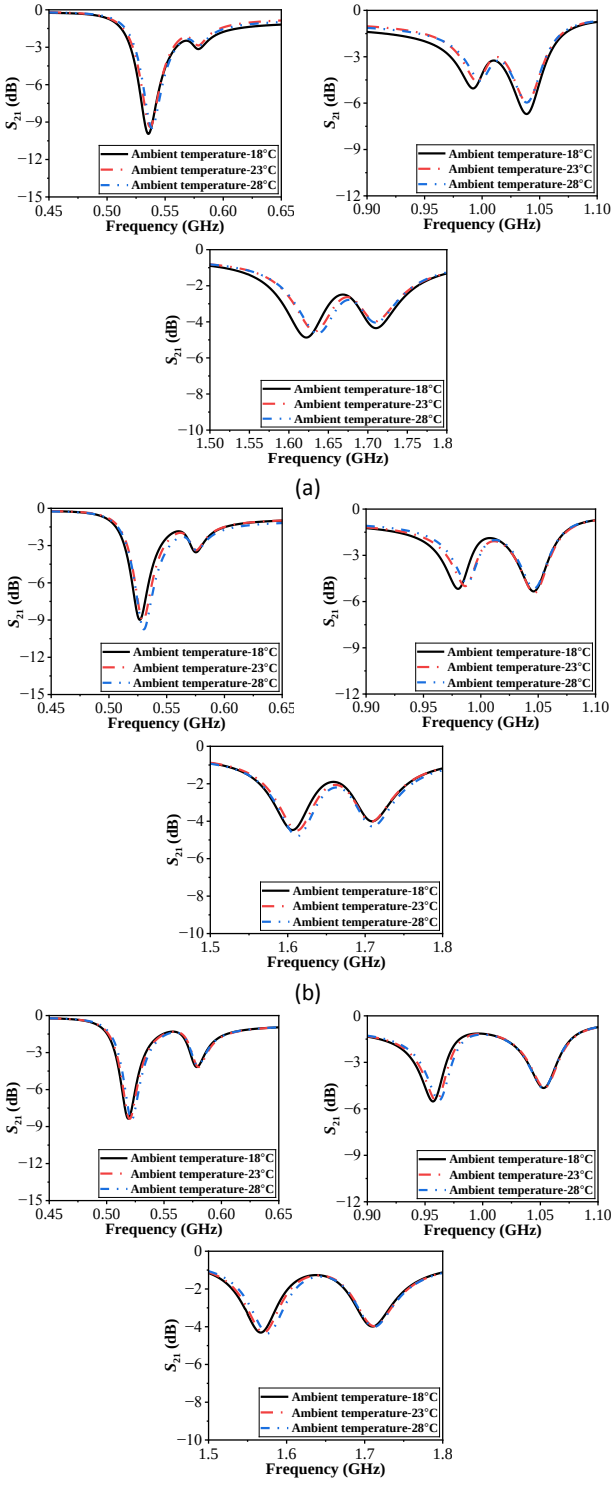

(a)

(b)

(c)

Fig. 11: Simulation results of ambient humidity variation for wheat grains at different MCs: (a) 10%, (b) 20%, (c) 30%.

For example, at 10% MC, $\acute{\epsilon}_r$ rises sharply from 1.64 at 25% ambient humidity to 1.95 at 45%, representing nearly a 19% increase. In contrast, at 30% MC, $\acute{\epsilon}_r$ increases from 2.22 to 2.88 over the same ambient humidity range, corresponding to a relative change of only ~7%. This indicates that grains at lower MC are more sensitive to ambient humidity-induced dielectric variations, while those at higher MC approach saturation, leading to a reduced absorption rate. Consequently, samples with 10% MC exhibit the greatest sensitivity to environmental humidity fluctuations, whereas 20% and 30% MC samples show progressively lower sensitivity. Conversely, under lower ambient humidity, grains with low MC tend to lose water more rapidly than wetter grains due to a steeper vapor pressure gradient. This nonlinear sorption–desorption behavior aligns with grain storage studies and is crucial for interpreting microwave sensor data, as dielectric responses depend on both initial MC and ambient humidity.

Conclusion

This paper presented a high-sensitivity microwave sensor employing a differential measurement approach for effective MC monitoring. The sensor's operational principles were analyzed using odd- and even-mode theory, and its performance was validated through full-wave EM simulations. Simulated results showed strong agreement with experimental measurements. A prototype was fabricated on a low-cost FR-4 substrate and tested using wheat grain samples with varying MC levels. The measurement data confirmed that the sensor achieves a high average normalized sensitivity of 7.63%, demonstrating its accuracy and reliability for dielectric characterization. These findings highlight the sensor's suitability for practical deployment in food industry quality control, particularly in real-time grain MC monitoring applications.

Author Contributions

A. Bijari and S. Nooki collaboratively contributed to the analytical design of the sensor. A. Bijari developed the equivalent circuit model and derived the necessary analytical expressions. S. Nooki conducted the full-wave simulations and performed the experimental measurements. Both authors jointly analyzed the results and contributed to the writing of the manuscript.

Acknowledgment

The author gratefully acknowledges M. Eshghi for his valuable contribution to the PCB design.

Conflict of Interest

The authors declare no potential conflict of interest regarding the publication of this work. In addition, the ethical issues including plagiarism, informed consent, misconduct, data fabrication and, or falsification, double publication and, or submission, and redundancy have been completely witnessed by the authors.

Abbreviations

MC	Moisture Content
SUT	Sample Under Test
TZ	Transmission Zero
PCB	Printed Circuit Board
MW	Magnetic Wall
EW	Electric Wall
EM	Electromagnetic

References

[1] R. Keshavarz, J. Lipman, D. M.-P. Schreurs, N. Shariati, "Highly sensitive differential microwave sensor for soil moisture measurement," IEEE Sens. J., 21(24): 27458–27464, 2021.

[2] I. H. D. Belitz, W. Grosch, Food Chemistry. Berlin, Germany: Springer, 2013.

[3] R. N. Pereira, J. G. D. Júnior, M. E. T. S. Praxedes, K. C. Cabral, V. P. da Silva Neto, A. G. D'Assunção, "A planar DGS sensor for moisture analysis in civil construction aggregates," Sens. Actuators A Phys., 367: 115042, 2024.

[4] A. Beniwal, D. A. John, R. Dahiya, "PEDOT: PSS-based disposable humidity sensor for skin moisture monitoring," IEEE Sens. Lett., 7(3): 1–4, 2023.

[5] Y. I. Abdulkarim et al., "Utilization of a triple hexagonal split ring resonator (SRR) based metamaterial sensor for the improved detection of fuel adulteration," J. Mater. Sci.: Mater. Electron., 32(19): 24258–24272, 2021.

[6] L. Ali, G. Wang, F. Meng, X. Ding, K. K. Adhikari, C. Wang, "MXene-coated planar microwave resonator sensor for ultrasensitive humidity monitoring," IEEE Microw. Wireless Technol. Lett., 33(11): 1572–1575, 2023.

[7] S. S. Olokede, M. Chu, M. L. Neyestanak, M. Daneshmand, H. E. Naguib, "Non-recovery moisture sensor for breach integrity using the degenerate mode of planar microwave ring resonator," Sens. Actuators A Phys., 328: 112775, 2021.

[8] O. Altintas, M. Aksoy, E. Unal, F. Karakasli, M. Karaaslan, "A split meander line resonator-based permittivity and thickness sensor design for dielectric materials with flat surface," J. Electron. Mater., 47: 6185–6192, 2018.

[9] M. Bakır et al., "High sensitive metamaterial sensor for water treatment centres," Water Air Soil Pollut., 230: 1–9, 2019.

[10] D. K. Ghodgaonkar, V. V. Varadan, V. K. Varadan, "A free-space method for measurement of dielectric constants and loss tangents at microwave frequencies," IEEE Trans. Instrum. Meas., 38(3): 789–793, 1989.

[11] F. Lu, Q. Tan, Y. Ji, Q. Guo, Y. Guo, J. Xiong, "A novel metamaterial inspired high-temperature microwave sensor in harsh environments," Sensors, 18(9): 2879, 2018.

[12] S. Jain, P. K. Mishra, V. V. Thakare, J. Mishra, "Microstrip moisture sensor based on microstrip patch antenna," Prog. Electromagn. Res. M, 76: 177–185, 2018.

[13] N. Javanbakht, G. Xiao, R. E. Amaya, "Portable microwave sensor based on frequency-selective surface for grain moisture content monitoring," IEEE Sens. Lett., 5(11): 1–4, 2021.

[14] H. K. Mun, K. Y. You, M. N. Dimon, "Rice grain moisture determination using microstrip wide-ring and microstrip coupled-line sensors," Am. J. Appl. Sci., 12(2): 112–120, 2015.

[15] A. Kapoor, P. K. Varshney, M. J. Akhtar, "Interdigital capacitor loaded electric-LC resonator for dielectric characterization," Microw. Opt. Technol. Lett., 62(9): 2835–2840, 2020.

[16] M. Shahbandeh "Worldwide production of grain in 2024/25," Statista, [Online].

[17] J. S. Hong, M. J. Lancaster, Microstrip Filters for RF/Microwave Applications, 2nd ed. Hoboken, NJ, USA: Wiley, 2011, pp. 7–28.

[18] V. K. Tripathi, "Asymmetric coupled transmission lines in an inhomogeneous medium," IEEE Trans. Microw. Theory Techn., 23(9): 734–739, 1975.

[19] S. Kal, D. Bhattacharya, N. B. Chakraborti, "Normal-mode parameters of microstrip coupled lines of unequal width (Short Paper)," IEEE Trans. Microw. Theory Techn., 32(2): 198–200, 1984.

[20] I. J. Bahl, S. S. Stuchly, "Analysis of a microstrip covered with a lossy dielectric," IEEE Trans. Microw. Theory Techn., 28(2): 104–109, 1980.

[21] K. E. Ileleji, A. A. Garcia, A. R. Kingsly, C. L. Clementson, "Comparison of standard moisture loss-on-drying methods for the determination of moisture content of corn distillers dried grains with solubles," J. AOAC Int., 93(3): 825–832, 2010.

[22] A. Ebrahimi, J. Scott, K. Ghorbani, "Differential sensors using microstrip lines loaded with two split-ring resonators," IEEE Sensors J., 18(14): 5786–5793, 2018.

[23] A. Ebrahimi, J. Scott, K. Ghorbani, "Transmission lines terminated with LC resonators for differential permittivity sensing," IEEE Microw. Wireless Compon. Lett., 28(12): 1149–1151, 2018.

[24] A. Ebrahimi, G. Beziuk, J. Scott, K. Ghorbani, "Microwave differential frequency splitting sensor using magnetic-LC resonators," Sensors, 20(4): 1066, 2020.

[25] P. K. Varshney, A. Kapoor, M. J. Akhtar, "Highly sensitive ELC resonator based differential sensor," IEEE Trans. Instrum. Meas., 70: 1–10, Art no. 8004710, 2021.

[26] W. J. Wu, W. S. Zhao, "A differential microwave sensor loaded with magnetic-LC resonators for simultaneous thickness and permittivity measurement of material under test by odd- and even-mode," IEEE Sensors J., 23(12): 12808–12816, 2023.

[27] S. Jiang, G. Liu, M. Wang, Y. Wu, J. Zhou, "Design of high-sensitivity microfluidic sensor based on csrr with interdigital structure," IEEE Sensors J., 23(16): 17901–17909, 2023.

[28] Z. Li, S. Tian, J. Tang, W. Yang, T. Hong, H. Zhu, "High-sensitivity differential sensor for characterizing complex permittivity of liquids based on LC resonators," Sensors, 24(15): 4877, 2024.

[29] M. T. Khan, X. Q. Lin, A. M. Khan, Z. Chen, "Sensitivity enhancement for moisture content detection using modified microstrip patch antennas," AIP Advances, 14(5): 055219, 2024.

[30] J. Yeo, J. I. Lee, "Design of a high‐sensitivity microstrip patch sensor antenna loaded with a defected ground structure based on a complementary split ring resonator," Sensors, 20(24), Art. no. 7064, 2020.

[31] C. G. Malmberg, A. A. Maryott, "Dielectric constant of water from 0 to 100 C," J. Res. National Bureau Standards, 56(1): 1-8, 1956.

Biographies

Abolfazl Bijari received his B.Sc. degree in Telecommunication Engineering, and his M.Sc. and Ph.D. degrees in Electronics Engineering from Ferdowsi University of Mashhad (FUM), Iran, in 2005, 2007, and 2013, respectively. He is currently an Associate Professor in the Department of Electronics Engineering at the University of Birjand, Iran. His research interests include RFIC design, microwave sensors, and MEMS devices.

- Email: a.bijari@birjand.ac.ir
- ORCID: 0000-0002-0552-0721
- Web of Science Researcher ID: AAP-6805-2020
- Scopus Author ID: 55000092200
- Homepage: https://cv.birjand.ac.ir/bijari/fa

Sara Nooki received her B.Sc. degree in Biomedical Engineering from Islamic Azad University (IAU) of Birjand, Iran, in 2023, and her M.Sc. degree in Electronics Engineering from the University of Birjand, Iran, in 2025. Her research interests include microwave sensors.

- Email: sara.nooki@birjand.ac.ir
- ORCID: 0009-0003-4563-9924
- Web of Science Researcher ID: NA
- Scopus Author ID: NA
- Homepage: NA